Chapter 11: Multiscale Modeling of the Evolution of Damage in Heterogeneous Viscoelastic Solids

David H. Allen and Roberto F. Soares

University of Nebraska-Lincoln, Lincoln, NE 68520, USA

11.1 Introduction

It has long been recognized that one of the primary failure modes in solids is due to crack growth, whether it be a single or multiple cracks. It is known, for instance, that Da Vinci [14] proposed experiments of this type in the late fifteenth century. Indeed, modern history is replete with accounts of events wherein fracture-induced failure of structural components has caused the loss of significant life. Such events are common in buildings subjected to acts of nature, such as earthquakes, aircraft subjected to inclement weather, and even human organs subjected to aging. Therefore, it would seem self-evident that cogent models capable of predicting such catastrophic events could be utilized to avoid much loss of life. However, despite the fact that such events occur regularly, the ability to predict the evolution of cracks, especially in inelastic media, continues to elude scientists and engineers. This appears to be at least due, in part, to two as yet unresolved issues (1) there is still no agreed upon model for predicting crack extension in inelastic media and (2) the prediction of the extension of multiple cracks simultaneously in the same object is as yet untenable.

While it would be presumptuous to say that the authors have resolved these two outstanding issues, there is at least a glimmer of hope that these two issues may be resolved by using an approach not unlike that proposed herein. This chapter outlines an approach for predicting the evolution of multiple cracks in heterogeneous viscoelastic media that ultimately leads to failure of the component to perform its intended task. Examples of such components would include geologic formations, cementitious roadways,

human organs, and advanced structures, including composite aircraft components and defensive armor such as that used on tanks. Implicit in the need for deploying such a model as that proposed herein are the following two requirements (1) at least some subdomain of the medium must be inelastic and (2) cracks must grow on at least two significantly different length scales prior to failure of the component.

The model that is proposed herein for addressing this problem is posed entirely within the confines of the fundamental assumption embodied in continuum mechanics, i.e., that the mass density of a body is continuously differentiable in spatial coordinates on all length scales of interest so that cracks that initiate on the scale of single atoms or molecules cannot be modeled by this approach, implying that the smallest scale that can be considered is of the order of tens to hundreds of nanometers.

This chapter opens with a short historical review of developments that have led up to the current state of knowledge on this subject, followed by a detailed description of the methodology proposed by the authors for addressing this problem. This will be followed by a few example problems that are meant to illustrate how the approach described herein can be utilized to make predictions of practical significance.

11.2 Historical Review

The discipline of mechanics, the study of the motion of bodies, dates to the ancients. Chief among these is Archimedes [32], who enunciated the principle of the lever among other achievements. However, the first systematic study of the mechanics of bodies is attributed to Galileo [19] in the early seventeenth century. These accomplishments were not withstanding, it was not until the early nineteenth century that concerted efforts were made to study the motions of *deformable* bodies within the context of continuum mechanics. These efforts appear to have been initiated with the study of plates by Germain [20] and were followed shortly thereafter by the seminal papers by Navier [26] and Cauchy [10] on the prediction of deformations in elastic bodies. These formulations utilized Newton's laws of motion [27], together with definitions of strain and the necessary idea of the constitution of an elastic body, first enunciated by Hooke [8], a contemporary of Newton. These initial formulations did not encompass the notion of dissipation of energy, so the prediction of failure was not a component of these models. However, over the course of the succeeding century, the formulation of fundamental concepts of thermodynamics led to the first cogent theory of fracture by Griffith [21] in 1920.

Griffith proposed that a crack would extend in an elastic body whenever

$$G \geq G_C, \tag{11.1}$$

where G is the energy released per unit area of crack produced and G_C is assumed to be a material constant called the *critical energy release rate*.

Though succeeding progress has been slow to develop, this monumental proposition seems to have been the key step that was necessary to begin to make somewhat accurate predictions of crack growth. Two obstacles lay in the way before the usefulness of Griffith's proposition could be ascertained. The first obstacle was centered around the right-hand side of inequality (11.1): how to measure the material property required to make cogent predictions. The answer to this question was suggested in a paper by Rice [29] and proven mathematically a decade later by Gurtin [22]. Subsequently, techniques have been developed for quite accurately measuring the critical energy release rate for a broad range of materials. The other obstacle arose due to the left-hand side of inequality (11.1): how to accurately *calculate* the available energy in a body necessary to produce new crack surface area. This issue is complicated by the fact that, in an imaginary elastic body, it is necessary for the stresses at a crack tip to be singular in order for there to be a nonzero energy available for crack extension. This problem has been studied in significant detail over the past half-century with some success. However, it would be presumptive to say that the subject is resolved; because in reality, it is not possible for the stresses at a crack tip to be singular.

Initial experimental results for brittle materials indicated that Griffith's proposition was accurate. However, when experimental results were obtained for ductile materials, such as crystalline metals, experimental results compared less favorably to predictions. For some time, efforts were made to improve upon the calculations of the available energy for crack growth in ductile materials; and to make these calculations, researchers turned to the more advanced constitutive theory, such as that embodied in plasticity theory [24]. However, it is now widely understood that Griffith's proposition is not accurate for some ductile materials due to the fact that energy dissipation occurs in a variety of ways other than crack extension, and in ways that depend on the history of loading of the body. In these circumstances, it may be more appropriate to envision the critical energy release rate G_c as a *history-dependent material property* rather than a material constant. In the meantime, other approaches have been developed, such as *cohesive zone models* [7, 16], that do not require the concept of a critical energy release

rate to predict crack extension (although energy release rates *can* be calculated by this approach); and these have met some success in modeling crack growth in ductile media.

Simultaneously, over the past half-century, two more or less contiguous developments have led to significant improvements in calculating the available energy for crack extension in both elastic and a variety of inelastic (including elastoplastic, viscoplastic, and both linear and nonlinear viscoelastic) media. One of these developments was the rise of the high-speed computer, whose power has made it possible to make billions of calculations of the type needed to estimate the energy required for crack extension, even in bodies of quite complicated geometry and material makeup. The other development is the finite element method, which grew out of the so-called *flexibility method* used in the aerospace and civil engineering communities in the first half of the twentieth century. This methodology came under scrutiny by the applied math community after World War II and was subsequently identified as a member of the *method of weighted residuals* for solving sets of coupled partial differential equations. Today, quite a few finite element codes are available for calculating stresses in both elastic and inelastic bodies.

11.3 The Current State of the Art

While significant progress has been made in the ability to predict when a crack will grow and where it will go, the subject has not yet been completely closed. As mentioned above, there is still no completely agreed upon way of predicting when a crack will grow in a ductile medium. Furthermore, when there are multiple cracks, the computational requirements needed to utilize the finite element method go up significantly. Even with today's high-speed computers, it is not yet possible to predict, with sufficient accuracy, the available energy for crack extension for the physical circumstance wherein a few cracks are simultaneously imbedded in a body. And yet, *it is known from experimental observation that many, many cracks can occur simultaneously in all manner of structural components and that these cracks can coalesce into a single crack that leads to structural failure*. It can be said here without reservation that the state of the art of fracture mechanics is not to the point where the evolution of large numbers of cracks of evenly distributed sizes in a single inelastic body can be predicted. However, there is one case involving multiple cracks that may be a tenable problem at this time. That is the case wherein the cracks in the body are distributed by size into widely separated length

scales, with a small number of cracks observed at the largest scale, termed the global or macroscale, upon which failure ultimately occurs. This, then, is the subject of this chapter: *to develop a modeling approach for predicting the evolution of multiple cracks on widely separated length scales in heterogeneous viscoelastic bodies*. To affect a solution technique, the problem will be solved by using the concept of *multiscaling*, as described below.

The concept of multiscaling in continuous media is an old one that is based on classical elasticity theory. In this approach, constitutive properties of the elastic object are required to predict deformations, stresses, and strains in a structural part. To obtain these properties, a *constitutive test* is performed on a specimen made of the material of interest. For the test to be valid, not only should the state of stress and strain in the body be measurable by observing boundary displacements of the object when it is loaded, but also it is necessary that the object be "statistically homogeneous." This is a sometimes ill-defined term; but what is meant by the term is that any asperities in the test specimen are several orders of magnitude smaller than the specimen itself, so that the spatial variations in the magnitudes of the observed stresses and strains in the test specimen are small compared to the mean stresses and strains observed during the test to obtain the constitutive properties. This type of experiment essentially embodies the concept of multiscaling. By *assuming* that the response of the test specimen is statistically homogeneous, the smaller length scale on which asperities might be observed is separated from the larger scale of the structural component.

This separation of length scales has long been understood, having been considered in some detail by nineteenth-century scientists such as Maxwell and Boltzmann, as well as in the early twentieth century by Einstein, to explain macroscale observations (visible to the naked eye) of molecular phenomena in liquids and gases. Capitalizing on this approach, a number of researchers developed rigorous mathematical techniques in the 1960s for bounding the elastic properties of multiphase elastic continua [17, 23, 25]. Such methods earned the descriptor "micromechanics," although this designator is perhaps not the best terminology, since the observed heterogeneity is often not microscopic. Nevertheless, this approach has gained acceptance as a means of estimating the elastic properties of objects composed of multiple elastic phases which are small compared to the size of the body of interest. The advantage of such models (over the experimental approach described above) for measuring elastic properties is that the volume fractions (as well as shape, orientations, etc.) of the constituents can be changed without the necessity of redoing sometimes costly constitutive experiments. Thus, this approach, that inherently involves multiscaling, has

become quite popular in the engineering field. Furthermore, because the resulting body is elastic, the analyses on the smaller and larger scales can be performed independently of one another, so that no coupling between the two-length scales is necessary.

In the case of inelastic media, this, unfortunately, is not the case. When materials undergo load-induced energy dissipation, such as that occurs in elastoplastic or viscoelastic media, the micromechanical description does not decouple from the analysis to be performed on the larger scale. In other words, the material properties become spatially variable and dependent on the load history, so that coupling between the macro- and microscale is unavoidable. Therefore, it becomes essential to develop modeling approaches that account for this fundamental increase in the level of complexity of the problem if there is to be any hope of achieving accuracy of prediction.

For the better part of the last half of the twentieth century, efforts to account for this complexity in inelastic media centered on development of ever more complicated constitutive theories for the microscale, similar to that used successfully to model heterogeneous elastic media, as described above. This had the pragmatic basis that one could perform a finite element analysis on a single length scale, which was just about the limit that computers of that time could handle. However, as it became apparent that microscale cracking would have to be included in constitutive models of heterogeneous media at the macroscale, efforts began to bog down and become very complicated indeed. To account for observed behavior in test specimens with time-dependent microcracking, more and more (often unexplained) phenomenological parameters had to be introduced into models. This approach developed the name “continuum damage mechanics.” It also inherited the unpalatable complication that sometimes many experimentally measured material parameters were required, especially when it became necessary to model *evolving* microcracks.

Enter the twenty-first century and more and more powerful computers. What required a supercomputer 10 years ago now requires only a desktop computer. Therefore, it is now possible to conceive of algorithms that obviate the necessity to perform many complicated experiments at the microscale. Furthermore, these new algorithms have the added advantage that, by performing simultaneous computations on both the micro- and global scales, they possess the flexibility to include heretofore unmanageable design variables at the microscale in the global design process, and without recourse to expensive constitutive testing.

11.4 Multiscale Modeling in Inelastic Media with Damage

In this section, a multiscale model is proposed for predicting the evolution of damage on multiple scales in inelastic media. The formulation is taken from [5].

11.4.1 Microscale Model

Consider an approach proposed herein that can be used on any number of length scales l_μ observed in a solid object. The number of scales n utilized is determined by the physics of the problem on the one hand and the amount of computational speed and size available on the other hand. To that end, consider a solid object with a region wherein microcracks are evolving on the smallest length scale considered l_1, as shown in Fig. 11.1.

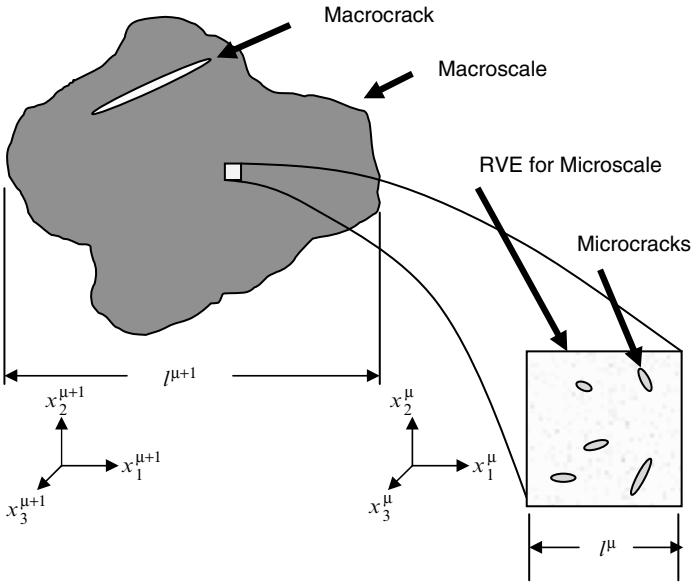

Fig. 11.1. Scale problem with cracks on both length scales

While it is not necessary (or even always correct) that a representative volume of the object on this length scale be accurately modeled by continuum mechanics, it is assumed that this is the case in this chapter to simplify the discussion. Suppose that the object can be treated as linear viscoelastic, again for simplicity, so that the following initial–boundary value problem (IBVP) may be posed.

Conservation of linear momentum

$$\vec{\nabla} \cdot \tilde{\sigma}_{\mu} + \rho \vec{f} = 0, \quad \forall \vec{x}_{\mu} \in V_{\mu}, \tag{11.2}$$

where $\tilde{\sigma}_{\mu}$ is the Cauchy stress tensor defined on length scale μ, ρ is the mass density, and $\vec{f}$ is the body force vector per unit mass. Note that inertial effects have been neglected, implying that the length scale of interest is small compared to the next larger length scale, thus neglecting the effects of waves at this scale on the next scale up. Ultimately, it will be convenient within this context to model waves only on the largest, or global, scale.

Strain–displacement equations

$$\tilde{\varepsilon}_{\mu} \equiv \frac{1}{2}[\vec{\nabla}\vec{u}_{\mu} + (\vec{\nabla}\vec{u}_{\mu})^{\mathrm{T}}], \tag{11.3}$$

where $\tilde{\varepsilon}_{\mu}$ is the strain tensor on the length scale μ and $\vec{u}_{\mu}$ is the displacement vector on the length scale μ. Note that the linearized form of the strain tensor has been taken for simplicity, although a nonlinear form may be employed without loss of generality.

Constitutive equations

$$\tilde{\sigma}_{\mu}(\vec{x}_{\mu}, t) = \Omega_{\tau=-\infty}^{\tau=t}\{\tilde{\varepsilon}_{\mu}(\vec{x}_{\mu}, \tau)\}, \tag{11.4}$$

where $\vec{x}_{\mu}$ is the coordinate location in the object on the length scale μ, which has interior V_{μ} and boundary ∂V_{μ}.

The above description implies that the entire history of strain at any point in the body is mapped into the current stress, which is termed a *viscoelastic material model*. Because only the value of strain (the symmetric part of the deformation gradient is used in this model) is required at

the point of interest, it is sometimes called a simple (or local) model [15]. Note that a local elastic material model, such as Hooke's law [32], is a special case of (11.4).

Equations (11.2)–(11.4) must apply in the body, together with appropriate initial and boundary conditions. These are then adjoined with a fracture criterion that is capable of predicting the growth of new or existing cracks anywhere in the object. There are multiple possibilities but, for example, the Griffith criterion given by inequality (11.1) can be taken. The above then constitutes a well-posed boundary value problem, albeit nonlinear due to the crack growth criterion (perhaps as well as the constitutive model (11.4)).

Obtaining solutions for this problem, even for simple geometries, is in itself a difficult challenge, as anyone who has every attempted to do so will attest. Nevertheless, assume that by some means (most likely computational) a solution can be obtained for the boundary conditions, geometry, and precise form of the constitutive (11.4) at hand. Assume, furthermore, that the cracks that are predicted within the model dissipate so much energy locally that they may have further deleterious effects on the response at the next larger length scale. As an example, the so-called *microcracks* may in some way influence the development or extension of one or more macrocracks on the next larger length scale l_2. It will be assumed that the cracks on the next larger length scale are much larger than those on the current scale and that this restriction applies to all length scales for cracks in the object of interest

$$l_{\mu+1} \gg l_\mu, \quad \mu = 1, \ldots, n, \tag{11.5}$$

where n is the number of different length scales observed in the solid.

Note that the above restriction is a *necessary condition* (but not sufficient) for the multiscale methodology proposed herein to produce reasonably accurate predictions on the larger length scale(s). If this condition is not satisfied, as in the case of a so-called *localization problem*, then there may indeed be no alternative to performing an exhaustive analysis at a single scale that takes into account all of the asperities simultaneously.

11.4.2 Homogenization Principle Connecting the Microscale to the Macroscale

To perform an analysis of the solid on the next length scale up from the local scale (termed the macroscale herein for simplicity), it is necessary to find a means of linking the state variables predicted on the microscale to

those on the macroscale. Of course, the state variables at the microscale are predicted at an infinite collection of material points in the local domain $V_\mu + \partial V_\mu$, so that there is plenty of information available to supply to the next larger length scale. However, the objective herein is to find an efficient means of constructing this link without sacrificing too much accuracy. In other words, it is propitious to utilize the minimum data obtained at the local scale necessary to make a sufficiently accurate prediction at the macroscale. One way is to link the microscale to the macroscale via the use of mean fields. To see how this might work, consider the following mathematical expansion for the macroscale stress in terms of the microscale stress

$$\tilde{\sigma}_{\mu+1} = \bar{\bar{\tilde{\sigma}}}_\mu + \sum_{j=1}^{\infty} \frac{1}{V_\mu \left|\bar{\vec{x}}\right|^j} \int_{V_\mu} \left(\tilde{\sigma}_\mu - \bar{\bar{\tilde{\sigma}}}\right) \left|\vec{x}\right|^j \, \mathrm{d}V, \tag{11.6}$$

where

$$\bar{\bar{\tilde{\sigma}}}_\mu \equiv \frac{1}{V_\mu} \int_{V_\mu} \tilde{\sigma}_\mu \mathrm{d}V \tag{11.7}$$

is the volume averaged (or mean) stress at the microscale, and it is assumed that the local coordinate system is set at the geometric centroid of the microscale volume.

Note that, since the microscale domain $V_\mu + \partial V_\mu$ can be placed arbitrarily within the domain on the next larger length scale $V_{\mu+1} + \partial V_{\mu+1}$, the mean stress $\bar{\bar{\tilde{\sigma}}}_\mu$ is a continuously varying function of coordinates $\vec{x}_{\mu+1}$ on the next larger length scale $\mu + 1$, as shown in Fig. 11.1. Note also that the terms within the summation in (11.6) represent higher area moments of the stress tensor.

Now, it may be said without loss of generality that microscale conservation of momentum (11.2) also applies to the macroscale (assuming that quasistatic conditions still hold at this length scale)

$$\vec{\nabla} \cdot \tilde{\sigma}_{\mu+1} + \rho \vec{f} = 0, \quad \forall \vec{x}_{\mu+1} \in V_{\mu+1}. \tag{11.8}$$

By using (11.6), it can be shown that

$$\lim_{l_\mu / l_{\mu+1} \to 0} (\tilde{\sigma}_{\mu+1}) = \bar{\bar{\tilde{\sigma}}} \tag{11.9}$$

and (11.8) reduces to the following:

$$\vec{\nabla} \cdot \bar{\bar{\tilde{\sigma}}}_\mu + \rho \vec{f} = 0, \quad \forall \vec{x}_{\mu+1} \in V_{\mu+1}. \tag{11.10}$$

The similarity between (11.2) and (11.10) is sufficiently striking that one is immediately tempted to use the same modeling algorithm on both length scales (note that if the momentum terms on the right-hand side of (11.8) are not negligible at the macroscale, then a different algorithm must be used at this length scale, as will be discussed below). This indeed is the approach that will be taken herein; but it must necessarily be said that (11.10) is only exact in the limit, i.e., (11.9) is a *sufficient condition* for (11.10) to be exact. However, in all real circumstances, (11.9) cannot be satisfied, so that some error must necessarily be introduced by utilizing approximate (11.10) in lieu of exact (11.10).

The use of (11.10) is termed herein a "mean field theory" because the higher-order terms that are dropped from (11.6) are essentially higher area moments of the microscale stress. Thus, the macroscale analysis is performed only in terms of the mean stress $\bar{\tilde{\sigma}}$. Note that, in cases wherein there is localization induced by damage or large strain gradients, one or more of the higher-order terms will not be negligible. In this case, a mean field theory is no longer accurate; and a nonlocal approximation (including one or more of the higher-order terms in (11.6)) or even a full field analysis performed simultaneously on all length scales may be necessary to obtain reasonable accuracy. However, the necessity for converting to this procedure may be monitored by calculating the higher-order terms in (11.6) after each time step during the local scale analysis.

Now consider the standard deviation of the microscale stress, given by

$$\tilde{\sigma}_{\mu}^{\mathrm{SD}} \equiv \frac{1}{V_{\mu}} \int_{V_{\mu}} \left(\tilde{\sigma}_{\mu} - \bar{\tilde{\sigma}}_{\mu} \right)^2 \mathrm{d}V. \tag{11.11}$$

An object in which the standard deviation of all of the state variables is small compared to their respective means is termed, in this chapter, "statistically homogeneous" (this, of course, implies that the effects of any singularities are bounded when integrated over the volume). It can also be shown that, when (11.9) is satisfied, the standard deviation of the microscale stress, given by (11.11), goes to zero. Therefore, in many cases it is sufficient for the object to be statistically homogeneous at the microscale in order for (11.10) to be an accurate representation at the macroscale. One implication of this result is that the microcracks contained within the microscale volume must be statistically homogeneous in location and orientation. If this is not the case, then higher-order moments will necessarily have to be included at the macroscale [1].

Now note that, as long as any tractions on the crack faces are self-equilibrating, (11.2) may be used to show that [6, 9, 13]

$$\bar{\tilde{\sigma}}_{\mu} = \frac{1}{V_{\mu}} \int_{\partial V_{\mu}} (\tilde{\sigma}_{\mu} \cdot \vec{n}_{\mu}) \vec{x}_{\mu} \mathrm{d}S, \tag{11.12}$$

where $\vec{n}_{\mu}$ is the unit outer normal vector on the local boundary ∂V_{μ}.

Note that the boundary averaged stress given in (11.12) actually is physically more palatable than the volume averaged stress given in (11.7), as it is commensurate with the original definition of stress, as defined by Cauchy [10], to act on a surface.

The fact that the volume averaged stress is equivalent to the boundary averaged stress is of little importance when there are no cracks. However, when cracks grow and evolve with time, it becomes a very important aspect of the homogenization process, as will now be shown by considering the homogenization process for the strain tensor. It can be shown by careful employment of the divergence theorem that

$$\bar{\tilde{\varepsilon}}_{\mu} = \tilde{\varepsilon}_{\mu+1} + \tilde{\alpha}_{\mu+1}, \tag{11.13}$$

where

$$\bar{\tilde{\varepsilon}}_{\mu} = \frac{1}{V_{\mu}} \int_{V_{\mu}} \tilde{\varepsilon} \, \mathrm{d}V \tag{11.14}$$

is the mean strain at the local scale,

$$\tilde{\varepsilon}_{\mu+1} = \frac{1}{V_{\mu}} \int_{\partial V_{\mu}^{\mathrm{E}}} \frac{1}{2} [\vec{u}_{\mu} \vec{n}_{\mu} + (\vec{u}_{\mu} \vec{n}_{\mu})^{\mathrm{T}}] \mathrm{d}S \tag{11.15}$$

is the boundary averaged strain on the initial (external) boundary of the local volume $\partial V_{\mu}^{\mathrm{E}}$, and

$$\tilde{\alpha}_{\mu+1} = \frac{1}{V_{\mu}} \int_{\partial V_{\mu}^{\mathrm{I}}} \frac{1}{2} [\vec{u}_{\mu} \vec{n}_{\mu} + (\vec{u}_{\mu} \vec{n}_{\mu})^{\mathrm{T}}] \mathrm{d}S \tag{11.16}$$

is the boundary averaged strain on the newly created (internal) boundary due to cracking $\partial V_{\mu}^{\mathrm{I}}$ and is called a *damage parameter* [17, 33].

Since kinematic equation (11.15) is consistent with kinetic equation (11.12), it is reasonable to construct constitutive equations at the macro-scale in terms of these two variables, rather than in terms of volume averages. This is in striking contrast to the approach taken when there are

no microcracks. In this case, there is no difference between boundary averages and volume averages, as can be seen from the above equations. Nevertheless, using (11.15) and the divergence theorem, it can be shown that

$$\tilde{\varepsilon}_{\mu+1} = \frac{1}{2}[\vec{\nabla}\vec{u}_{\mu+1} + (\vec{\nabla}\vec{u}_{\mu+1})^{\mathrm{T}}], \tag{11.17}$$

which can be seen to be similar in form to local equation (11.3).

The construction of a homogenized macroscale IBVP, similar to that posed in (11.2)–(11.4), is now nearly complete, as (11.10) replaces (11.2), and (11.17) replaces (11.3) at the macroscale. It remains to construct constitutive equations at the macroscale. Where one to utilize the continuum damage mechanics approach, it would be sufficient to simply postulate constitutive equations of the form:

$$\tilde{\sigma}_{\mu+1}(\vec{x}_{\mu+1}, t) = \Omega_{\tau=-\infty}^{\tau=t}\{\tilde{\varepsilon}_{\mu+1}(\vec{x}_{\mu+1}, \tau), \alpha(\vec{x}_{\mu+1}, \tau)\}. \tag{11.18}$$

The precise nature of this equation would then be determined by some curve-fitting scheme either to experimental data provided from macroscale experiments or the predictions made at the local scale. While this approach may be taken, as mentioned above, it removes the input parameters at the local scale from the design process. Therefore, it is preferable to take a multiscaling approach.

Instead, (11.18) is obtained by direct substitution of the microscale constitutive (11.4) into the volume averaged stress (11.7). The precise nature of the resulting equation will depend on the choice of a constitutive model. As an example, consider the case wherein the microscale constitutive behavior is linear nonaging viscoelastic

$$\tilde{\sigma}_{\mu}(\vec{x}_{\mu}, t) = \int_{-\infty}^{t} \tilde{\tilde{E}}_{\mu}(\vec{x}_{\mu}, t-\tau) \frac{\partial \tilde{\varepsilon}_{\mu}(\vec{x}_{\mu}, \tau)}{\partial \tau} \mathrm{d}\tau, \tag{11.19}$$

where $\tilde{\tilde{E}}(\vec{x}_{\mu}, t)$ is the relaxation modulus at the microscale.

Direct substitution of (11.19) into (11.7), and subsequent careful utilization of (11.6), (11.9), and (11.12)–(11.16), will result in a constitutive description at the macroscale that is of the following form [31]

$$\tilde{\sigma}_{\mu+1}(\vec{x}_{\mu+1}, t) = \int_{-\infty}^{t} \tilde{\tilde{E}}_{\mu+1}(\vec{x}_{\mu+1}, t-\tau) \frac{\partial \tilde{\varepsilon}_{\mu+1}}{\partial \tau} \mathrm{d}\tau, \tag{11.20}$$

where

$$\tilde{\tilde{E}}_{\mu+1}(\vec{x}_{\mu+1}, t) \equiv \int_{V_{\mu}} \tilde{\tilde{E}}(\vec{x}_{\mu}, t-\tau) \mathrm{d}V \tag{11.21}$$

is the volume average of the relaxation modulus at the microscale and is dependent on the damage incurred in the representative volume element at this scale, thereby implying that the material model described in (11.20) is nonlinear.

It is now apparent that macroscale equations (11.10), (11.13)–(11.16), and (11.19) correspond to microscale equations (11.2)–(11.4), so that a similar algorithm may be utilized for the analysis on both scales. The significant difference is that the introduction of cracks at the local scale results in a more complex and inherently nonlinear formulation of the constitutive equations at the macroscale. This then completes the description of the homogenization process and the resulting macroscale IBVP.

11.4.3 Cohesive Zone Model for Predicting Crack Growth on Each Length Scale

As mentioned in the historical review, there are several shortcomings of the Griffith criterion. First, it is often found to be inaccurate for viscoelastic media. Second, it is not convenient to utilize in a computational algorithm, which may be a necessary byproduct of modeling multiple cracks simultaneously. For these reasons, a different approach is taken herein for predicting crack growth in viscoelastic media. In this chapter, a cohesive zone model is utilized instead of the Griffith criterion. Models of this type are not new, having been introduced many years ago by Dugdale [16] and Barenblatt [7]. Initially, at least, a primary motivation of these models was to account for ductility that occurs in many materials, a phenomenon that is not generally captured well by the Griffith criterion. Unfortunately, cohesive zone models suffer from several shortcomings that have inhibited their deployment until recently. These are essentially related to the inability to measure directly the material parameters necessary to characterize a particular cohesive zone model. Furthermore, a cohesive zone model is normally deployed in such a way that it is necessary to know where the crack will propagate a priori. For these reasons, cohesive zone models are only now finding widespread usage.

On the other hand, cohesive zone models are endowed with several significant strengths. Firstly, they are quite conveniently deployable into a finite element code by simply joining two or more subdomains with self-equilibrating tractions, so that the domain may be treated as simply connected and then allowing the tractions to relax to zero as a function of one or more observed state variables during problem solution, thereby resulting in the production of new surface area. Secondly, cohesive zone models can be formulated in such a way that they can more accurately

capture fracture phenomena in some media than can the Griffith criterion. For example, it is often observed in viscoelastic media that the critical energy release rate required for crack extension is both rate and history dependent.

Recently, Allen and Searcy [2, 3, 4, 30] have produced a cohesive zone model for some viscoelastic media that is formulated in such a way that the material parameters required to characterize the cohesive zone model can be obtained directly from microscale experiments. Furthermore, this model is inherently two scale in nature, in that it utilizes the solution to a microscale continuum mechanics problem, together with a homogenization theorem, to produce a cohesive zone model on the next larger length scale. The model has also been shown to be consistent with advanced fracture mechanics, in that the cohesive zone requires a nonstationary critical energy release rate in order for a crack to propagate [11, 12, 33].

This model will not be reviewed in detail herein since it has already been reported in the literature; however, a brief review is given here. As shown in Fig. 11.2, the cohesive zone is postulated to be represented by a fibrillated or crazed zone that is small compared to the total cohesive zone area.

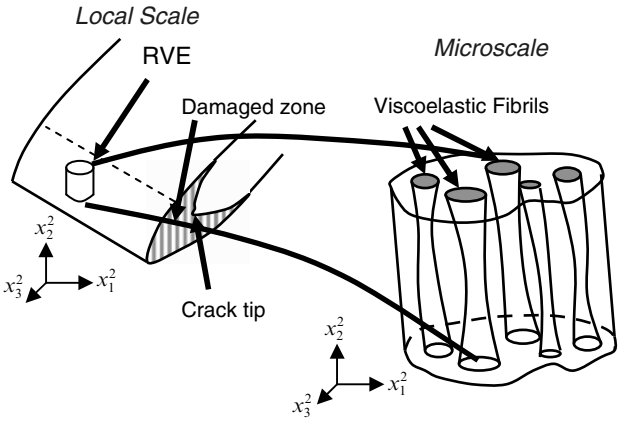

Fig. 11.2. Two-scale problem showing a cohesive zone at the microscale

The length scale of this IBVP is one-length scale below that of the smallest local scale required in the multiscale problem. In this chapter, the value $\mu = 1$ has been arbitrarily assigned to this length scale. The solution to this IBVP (with geometry as shown in Fig. 11.2 and governing equations identical to (11.2)–(11.4)) has been obtained and homogenized, thus leading to the following traction–displacement relation in the cohesive zone [3]

$$\vec{T} = \frac{\vec{\delta}}{\delta_0}(1-\alpha)\int_{\tau=0}^{\tau=1} E(t-\tau)\frac{\partial \lambda}{\partial \tau}\,\mathrm{d}\tau, \quad \forall \vec{x} \in \partial V_1, \tag{11.22}$$

where $E(t)$ is the uniaxial viscoelastic relaxation modulus of the undamaged cohesive zone material, ∂V_1 is the part of the boundary on which cohesive zones are active, $\vec{\delta}$ is the crack opening displacement vector in the coordinate system, aligned with the crack faces, λ is the Euclidean norm of the crack opening displacement vector, and α is the damage parameter, which in this case degenerates to a scalar, defined by

$$\alpha \equiv \frac{A_0 - \sum_{k=1}^{\mathrm{nf}} A_k}{A_0}, \tag{11.23}$$

where A_0 is the undamaged planform cross-sectional area of a representative area of the cohesive zone and nf is the number of fibrils contained in the representative area.

It can be seen that, when all of the fibrils in a representative area fracture, the damage parameter α goes to unity; and the traction vector in (11.20) becomes zero, thereby inducing crack propagation. Note that the damage parameter α does not exist on the smallest length scale. It appears as a natural byproduct of the homogenization process linking this scale to the next larger scale. This concept is not unlike the concept of temperature, which does not exist at the molecular scale but arises as an outcome of kinetic motions averaged up to the continuum scale. Thus, both are representations of the kinematics associated with entropy generation.

Note that herein the damage parameter for this scale is a scalar, unlike that produced at the other length scales, as defined in (11.16). This is due to the fact that, for the case of a cohesive zone, the homogenization process must be slightly altered to perform an area average rather than a volume average, as described in Sect. 11.4.2. In this case, the limit is taken as the dimension normal to the plane of the cohesive zone, which goes to zero, thereby reducing the *homogenized* cohesive zone to a traction–displacement relation rather than a stress–strain relation.

11.4.4 Formulation of Multiscale Algorithms

The approach detailed above may be used to develop multiscale algorithms for obtaining approximate solutions to problems containing multiple cracks growing simultaneously on widely differing length scales. This is accomplished by constructing a time-stepping algorithm in which the global

solution is first obtained for a small time step, assuming some initially damaged (or undamaged) state, as shown in Fig. 11.3. The global solution for this time step is then utilized to obtain solutions for each integration point at the local scale, using the state variables obtained as output from the global analysis to obtain the solution at the local scale. The results for each integration point are then homogenized to produce the global constitutive equations to be used on the next time step at the global scale. This procedure is essentially an operator splitting technique, assuming that there is one-way coupling between the two-length scales. Sufficient accuracy can usually be obtained by this method if successively smaller time steps are employed until convergence is obtained. Details of this approach may be found in [18, 34].

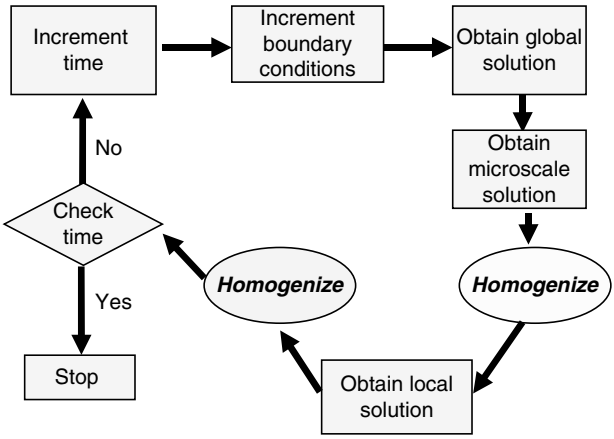

Fig. 11.3. Flowchart showing multiscale computational algorithm

In principle, the approach described herein can be utilized on as many (continuum) length scales as necessary to solve complex problems. However, the limits of continuum scales in nature ($10^{-10}\,\mathrm{m} < l < 10^{3}\,\mathrm{m}$), and the requirement that the length scales be broadly separated, as given by inequality (11.5), lead to the conclusion that only about five, or perhaps six, length scales are physically possible. On the other hand, depending on the complexity of the given problem, only about three *computational* scales are practical with current computer capacities. Fortunately, there are few problems of current technological significance that require more than about three computational scales (there is generally no limitation on the number of analytic scales, as these require little computation; but analytic

solutions, unlike the cohesive zone model described in Sect. 11.4.3, are not often attainable). Allen and coworkers have been able to obtain solutions on a desktop computer by this technique using as many as four scales simultaneously (although it must be admitted that two of the scales were analytical) [28]. For simplicity, a three-scale problem is illustrated in Fig. 11.4.

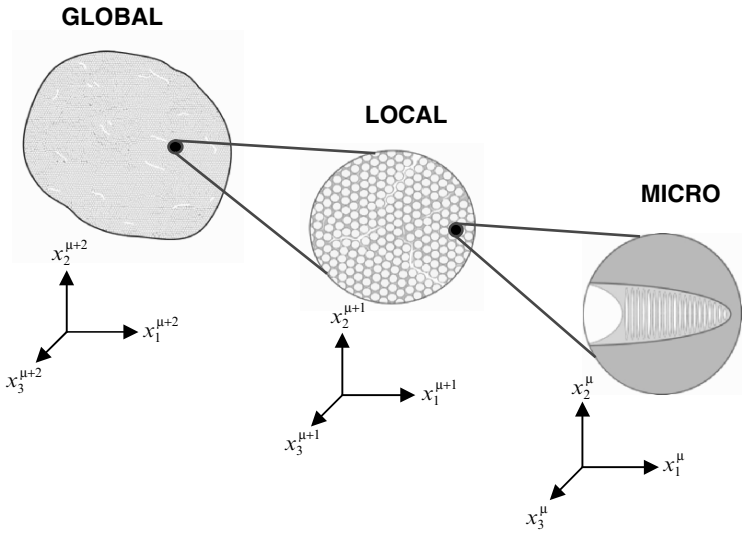

Fig. 11.4. Example of three-scale problem

11.5 Example Problems

In this section, two example problems are presented to demonstrate the technique of multiscaling with damage.

11.5.1 Tapered Bar Problem

The first problem to be considered is a uniaxial bar 10 m long and 2 m in depth with a linear varying cross-sectional area. Figure 11.5a shows the geometry of this tapered bar. The right end of the bar is subjected to a monotonically increasing load of 200 N in the x-direction, and displacements on the left end are restricted. In the local scale, the structure is

represented by a repeating unit cell, a square element with 0.025 m of side. This represents a quarter of one aggregate surrounded by asphalt material, shown in Fig. 11.5b. Cohesive zone elements are introduced in the interface between the aggregate and binder. As the load increases, the cohesive zones weaken and accumulate damage, leading to eventual crack growth on the local scale.

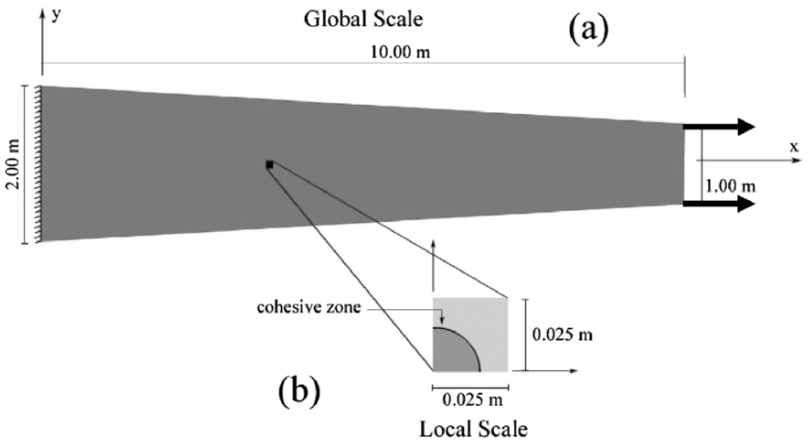

Fig. 11.5. (**a**) Global scale geometry and (**b**) local scale geometry

Symmetry along the *x*-direction in the global scale allows modeling of only half of the problem. The global scale finite element mesh is shown in Fig. 11.6a. The bar is discretized into 20 elements on the global scale; and each one of them is designated as a multiscale element, thus requiring a separate local analysis for each element in the global scale. The domain of the local scale is then partitioned into 12 triangular elements. A simple local mesh is then created with cohesive zone elements introduced in the interface between the aggregate and binder. The 20 undeformed local scale meshes at $t = 0$ are shown in Fig. 11.6b. Note that these are identical in the initial state but become different from one another as the damage accumulates.

As the bar is loaded, local elements experience differing damage accumulation according to their location, because the macroscale stresses increase toward the loaded end of the bar. Due to the fact that the bar is tapered, local elements close to the load undergo more damage than the ones away from the load.

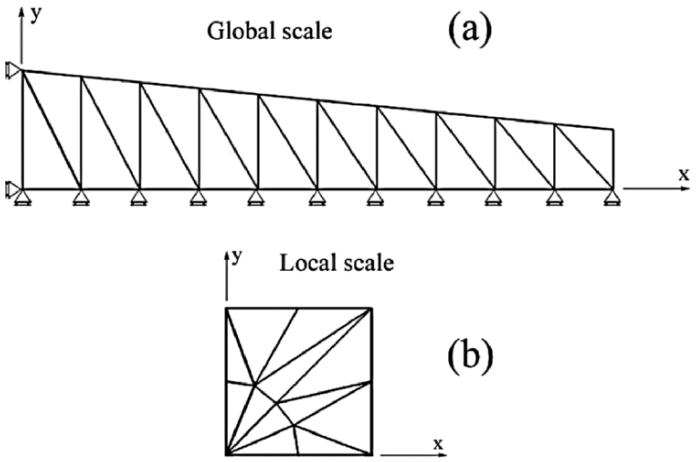

Fig. 11.6. Finite element global (**a**) and local (**b**) meshes of tapered bar

Table 11.1 shows the material properties for local and global meshes, as well as cohesive zone parameters. The bar is made of a hypothetical material model. All materials are assumed to be isotropic linear elastic, where δ_t and δ_n are material length parameter, A and n are damage parameters, and σ_n and σ_t are assumed to be zero.

Table 11.1. Material properties

Global		Local			
Bulk properties		Bulk properties		Cohesive zone properties	
E (Pa)	3.00×10^8	E (Pa)	3.00×10^8	E_∞ (Pa)	5.00×10^7
ν	0.35	ν	0.35	E_1 (Pa)	5.00×10^7
				η_1 (Pa s)	1.00×10^2
				ν	0.40
				δ_t (m)	1.00×10^{-3}
				δ_n (m)	1.00×10^{-3}
				A	0.1
				n	15

The applied force is illustrated in Fig. 11.7. A time increment of 1.0 s is used in this problem.

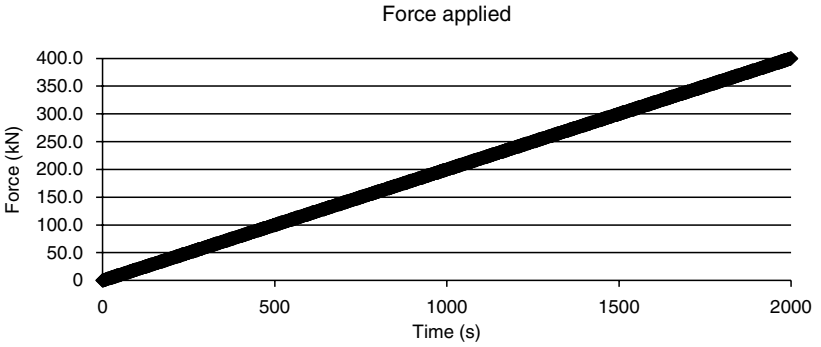

Fig. 11.7. Load applied

To illustrate the local behavior of the elastic tapered bar after the load is applied, the deformation of four different local meshes positioned at different locations along the bar are shown in different times. Four unit cells, chosen strategically within the global bar, are shown in Fig. 11.8. Those unit cells are shown in increments of 250 s, up to 1,000 s, in Fig. 11.9.

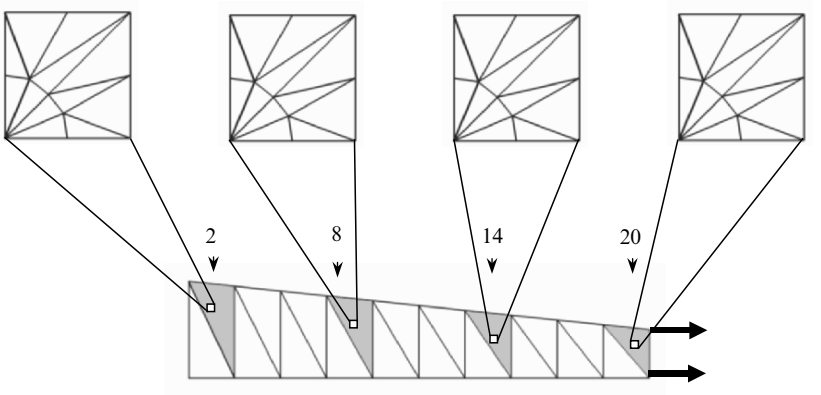

Fig. 11.8. Illustrated multiscale elements

The stress legend is positioned on the left side. It can be seen that all local elements start with zero stresses and no displacements. After 250 s, a cohesive zone opening can be seen in all but Element 2. At 500 s, a crack

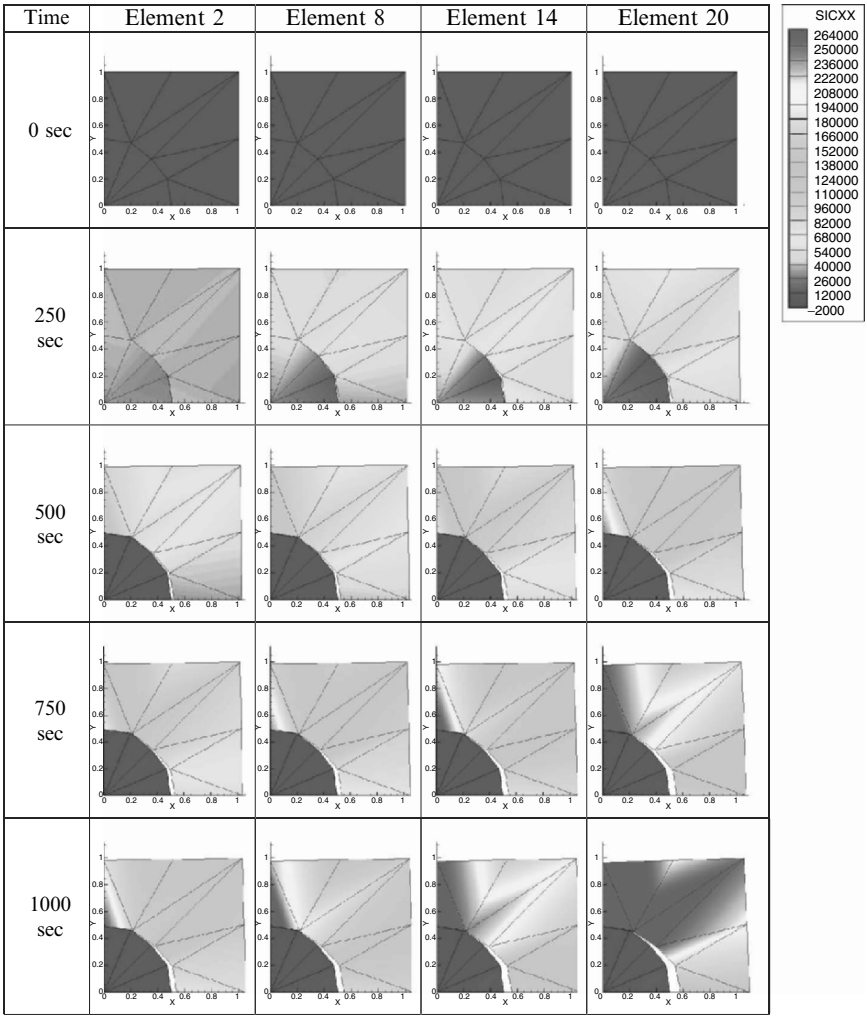

Fig. 11.9. Deformation of elastic tapered bar

has developed in all elements; and stresses are higher in Element 20. As the global force continues to increase and the time approaches 1,000 s, the stresses are still higher in Element 20; and the crack opening is also larger

in this element. This is expected to happen; since the cross-sectional area of the tapered bar is smaller on the right end, the global axial stresses are higher at this end. Figure 11.10 shows how the global scale evolves with time.

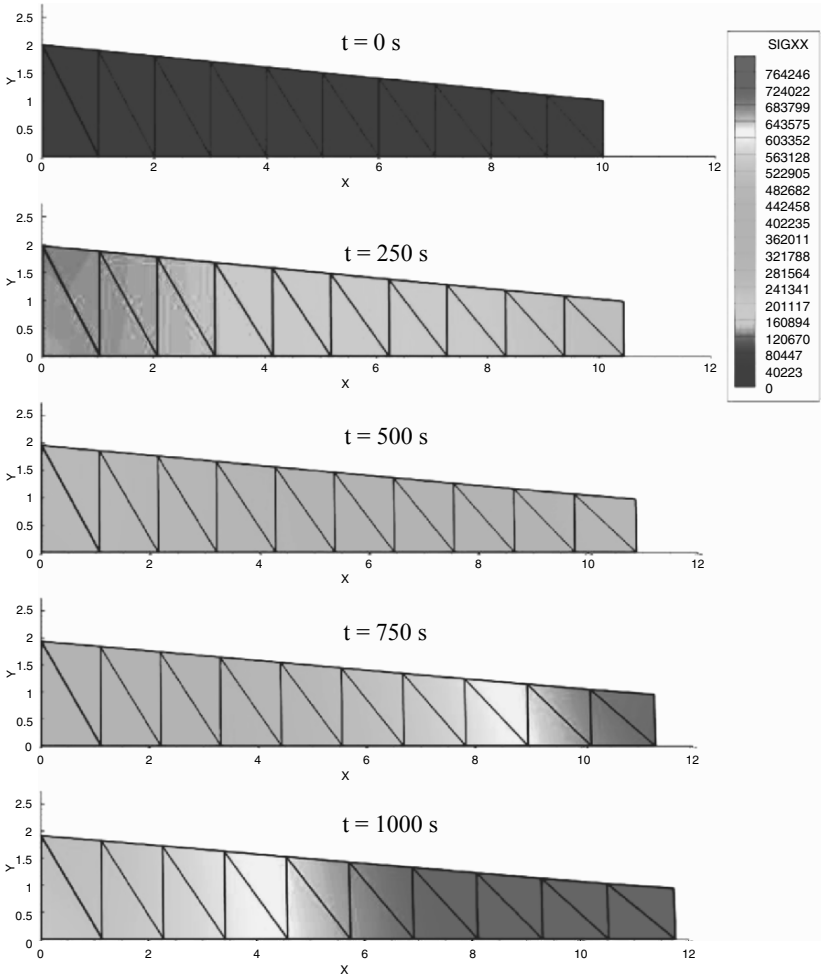

Fig. 11.10. Global deformation of elastic tapered bar

11.5.2 Roadway Problem

The next problem is an asphaltic roadway problem. This is an interesting multiscale problem which considers two different scales. The first step is to consider the geometry of the problem. Consider a typical two-lane asphalt roadway that contains a symmetry line down the middle of it, as shown in Fig. 11.11. For simplicity, only the right half of the pavement will be modeled. The road is 12 m wide with two 3.50 m traffic lanes and two shoulders of 2.50 m.

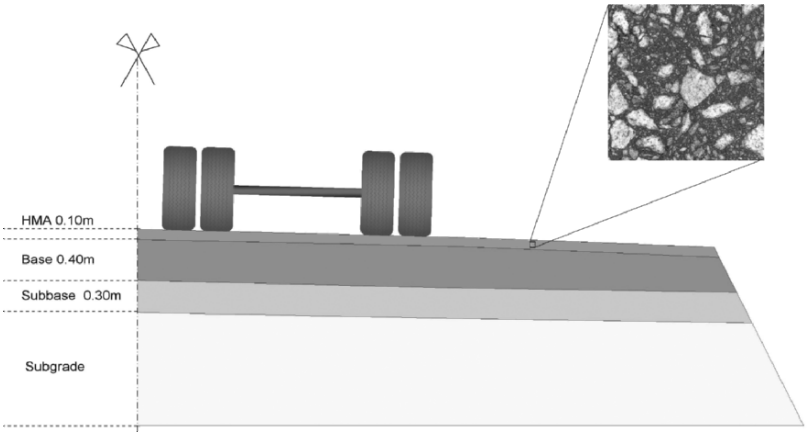

Fig. 11.11. Pavement geometry

The travel lane has slopes to both shoulders at 2% grade, while paved shoulders have slopes of 4%. Even though the pavement geometry can vary from case to case and require additional layers if necessary, the selected pavement for this analysis contains four layers. The top layer is a 10 cm hot mix asphalt, or HMA. The asphalt concrete layer is the final layer to be built on top of the other layers. The subsequent layers are made of granular material: a 40 cm granular base, a 30 cm granular subbase, and an in situ subgrade, which is the graded natural terrain and has a depth of 1.10 m in the model. All layers are modeled as isotropic elastic media. Table 11.2 shows material properties for all the layers.

Table 11.2. Material properties for each layer

	HMA	Base	Subbase	Subgrade
E (MPa)	14,500	4,000	800	200
ν	0.40	0.35	0.35	0.35

The local scale geometry is defined by scanning actual asphalt samples designed to perform laboratory tests. The global domain is discretized into 1,423 elements; the finite element mesh is shown in Fig. 11.12. Four global scale elements have been chosen for multiscale analysis. These elements are located in the surrounding area of the tire load.

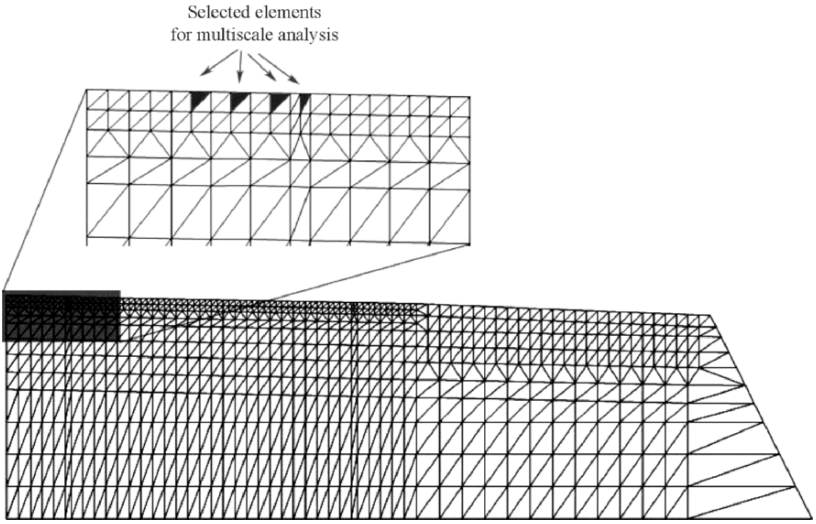

Fig. 11.12. Selected elements for multiscale analysis

The local scale problem was divided into 404 elements and is depicted in Fig. 11.13 in its undeformed configuration. The asphalt material and aggregate are both modeled as linear elastic material. Fracture, in the form of discrete cracks, is introduced at the local scale by 930 cohesive zone elements. All cohesive zone elements are located within the asphalt material; therefore, the interior of each aggregate does not possess any cohesive elements. Cohesive zone elements located in the interface of aggregate and asphalt imply that fracture will occur around the aggregate boundaries or by defibrillation of the asphalt.

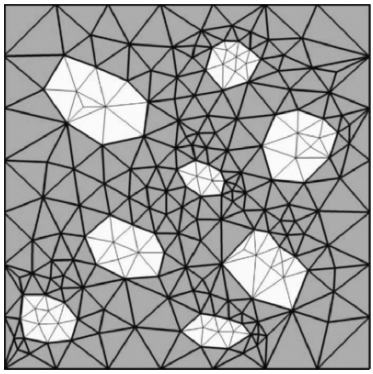

Fig. 11.13. Local scale mesh

Table 11.3 shows the material properties for all constituents of the local scale.

Table 11.3. Material properties for all constituents of the local scales

Local			
Bulk properties		Cohesive zone properties	
Asphalt		E_∞ (Pa)	5.00×10^7
E (Pa)	3.00×10^7	E_1 (Pa)	5.00×10^7
ν	0.35	η_1 (Pa s)	1.00×10^2
Rock		ν	0.40
E (Pa)	8.00×10^8	δ_t (m)	1.00×10^{-3}
ν	0.20	δ_n (m)	1.00×10^{-3}
		A	0.1
		n	15

For this analysis, the response of a cyclic load imposed by a truck on the pavement is simulated. The truck applies a static load of 151 kN with a tandem axle. A 60-ft. long truck traveling at 70 mph takes less than 1 s to pass through a fixed point on the pavement. However, for simplicity, 1 s of simulation was considered to simulate the passage of all five axles; ramp functions for axle loading and unloading were implemented in the code, with a period of 0.2 s for each passing axle or 0.1 s for loading and 0.1 s

for unloading, into a peak load of 18,900 kPa. The truck takes a total of five cycles of 0.2 or 1 s for all five axles, followed by a 19-s interval of rest, which is the time until the next truck passes, totaling a period of 20 s. Three trucks per minute or 180 trucks per hour are considered. Figure 11.14 shows the five axle loads and a rest period of up to 5 s, although the rest period still goes up to 20 s. For scale reasons, it would be hard to see the five cycles with a larger scale.

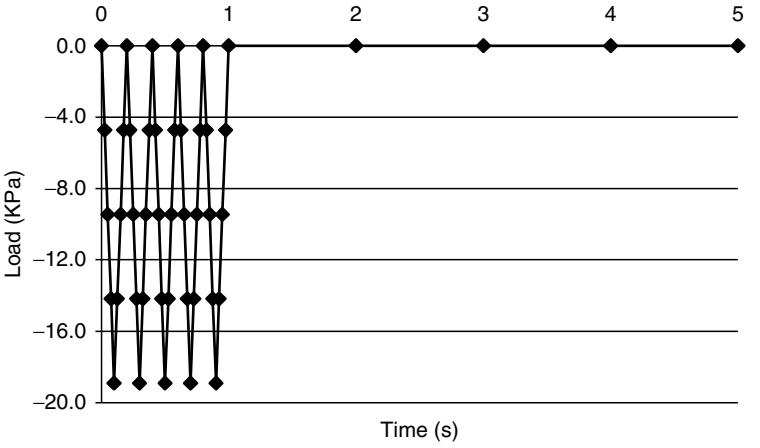

Fig. 11.14. Load history

Let us turn attention to the results of this multiscale problem. As shown in Fig. 11.12, four elements are selected for multiscale analysis; and the deformation of each of those elements as an outcome of the load applied is featured in Fig. 11.15.

It can be seen that, as time increases, elements on the edge of the load (Elements 11 and 23) accumulate less damage than the others with more direct action from the load (Elements 15 and 19). At $t = 0$, all unit cells have zero stresses; and as time progresses, Elements 15 and 19 suffer more damage because they are subjected to higher stresses. Figure 11.16 presents the global mesh with stress contours. It is possible to see that higher compressive stresses occur where the load is applied by the truck.

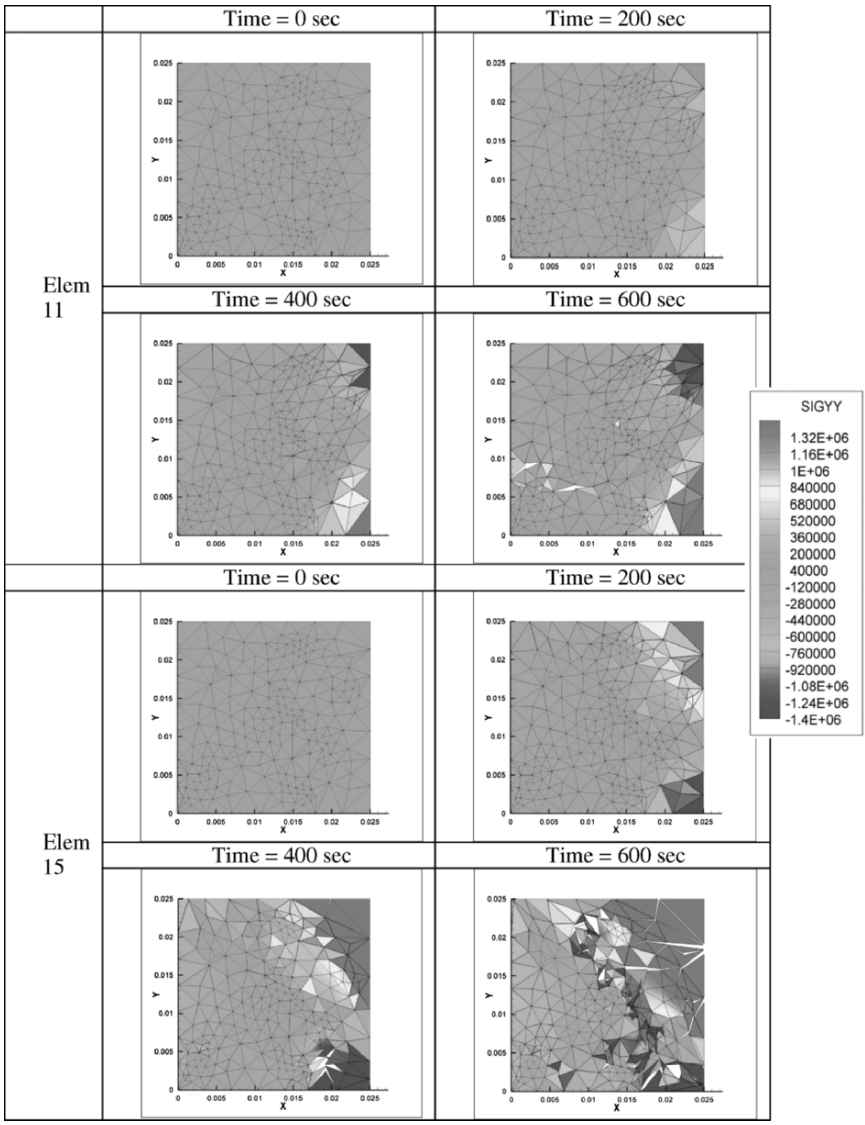

Fig. 11.15. Local deformation

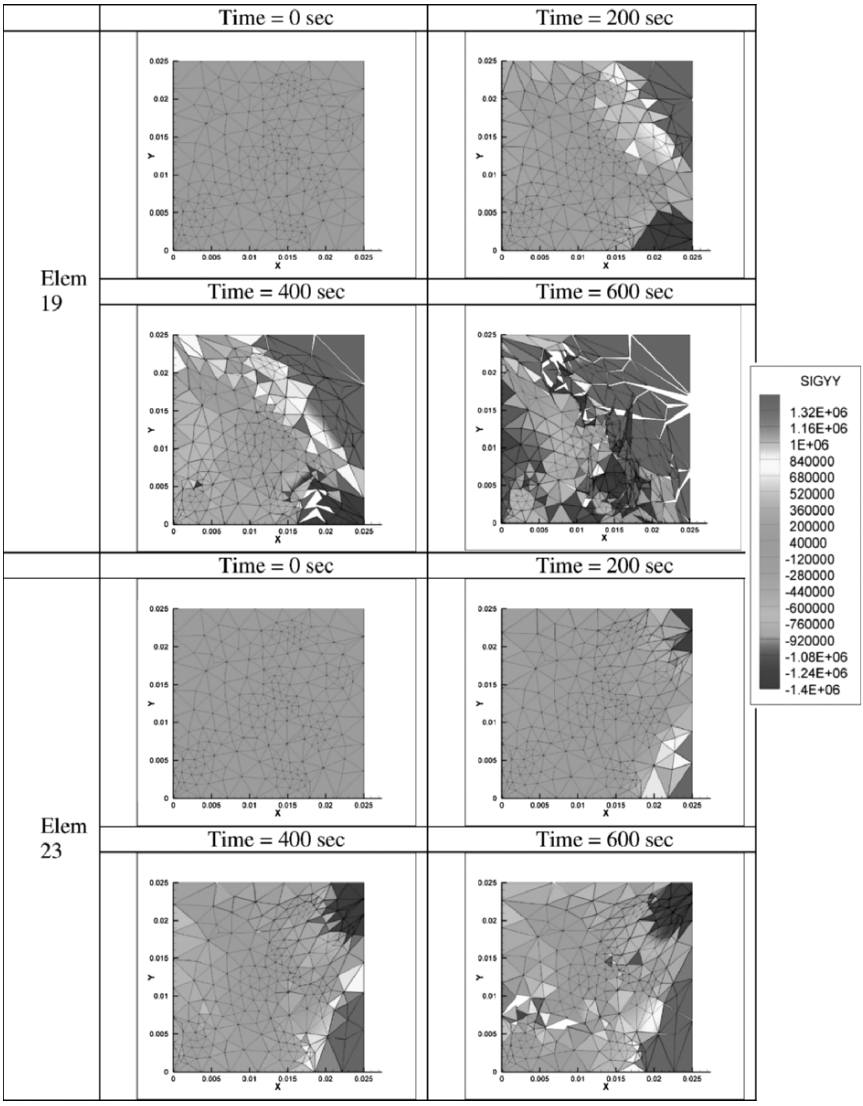

Fig. 11.15. *(cont'd)*

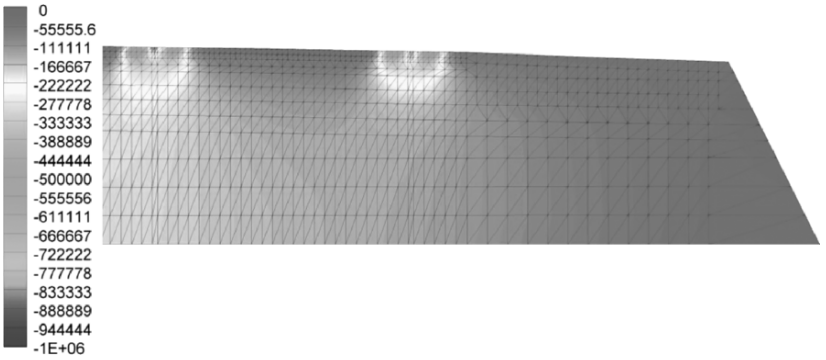

Fig. 11.16. Stress in global scale (*y* component)

11.6 Conclusion

A multiscale method has been developed for analysis of structural components that exhibit two or more length scales due to heterogeneity and/or evolving damage. The model is implemented into a finite element formulation, and the code employs a micromechanic, alloy-based, viscoelastic cohesive zone model to predict rate-dependent damage evolution.

Two simple example problems have been presented to facilitate the understanding of how the multiscale method works. Although further research is surely needed before this approach can be demonstrated to be accurate, it possesses the potential advantages that (1) material properties need be supplied only on the constituent scale, thereby simplifying the evaluation of material properties and (2) because material properties are specified at the constituent scale, variables, such as volume fraction of aggregate, can be readily incorporated into the design process.

Acknowledgment

The authors are grateful for funding received for this research from the U.S. Army Research Laboratory under contract No. W911NF-04-2-0011.

References

1. Allen, DH, Damage Evolution in Laminates, *Damage Mechanics of Composite Materials*, Talreja, R., Ed., Amsterdam: Elsevier, pp 79–114, 1994
2. Allen, DH, Homogenization Principles and Their Application to Continuum Damage Mechanics, *Composites Science and Technology* 61, 2223–2230, 2002
3. Allen, DH and CR Searcy, A Micromechanical Model for a Viscoelastic Cohesive Zone, *International Journal of Fracture* 107, 159–176, 2001
4. Allen, DH and CR Searcy, A Micromechanically-Based Model for Predicting Damage Evolution in Ductile Polymers, *Mechanics of Materials* 33, 177–184, 2001
5. Allen, DH and CR Searcy, A Model for Predicting the Evolution of Multiple Cracks on Multiple Length Scales in Viscoelastic Composites, *Journal of Materials Science* 41(20), 6510–6519, 2006
6. Allen, DH and C Yoon, Homogenization Techniques for Thermoviscoelastic Solids Containing Cracks, *International Journal of Solids and Structures* 35, 4035–4054, 1998
7. Barenblatt, GI, The Mathematical Theory of Equilibrium Cracks in Brittle Fracture, *Advances in Applied Mechanics* 7, 55–129, 1962
8. Bennett, J, Cooper, M, Hunter, M, and L Jardine, *London's Leonardo: The Life and Work of Robert Hooke*, Oxford: Oxford University Press, 2003
9. Boyd, JG, Costanzo, F, and DH Allen, A Micromechanics Approach for Constructing Locally Averaged Damage Dependent Constitutive Equations in Inelastic Composites, *International Journal of Damage Mechanics* 2, 209–228, 1993
10. Cauchy, AL, Recherches sur l'équilibre et le mouvement intérieur des corps solides ou fluides, élastiques ou non élastiques. *Bulletin de la Société philomatique* 9–13, 1823
11. Costanzo, F and DH Allen, A Continuum Mechanics Approach to Some Problems in Subcritical Crack Propagation, *International Journal of Fracture* 63(1), 27–57, 1993
12. Costanzo, F and DH Allen, A Continuum Thermodynamic Analysis of Cohesive Zone Models, *International Journal of Engineering Science* 33(15), 2197–2219, 1996

13. Costanzo, F, Boyd, JG, and DH Allen, Micromechanics and Homogenization of Inelastic Composite Materials with Growing Cracks, *Journal of the Mechanics and Physics of Solids* 44(3), 333–370, 1996
14. Da Vinci, Leonardo, *The Notebooks of Leonardo Da Vinci*, Richter, J.P., Ed., London: Jonathan Cape, 1970
15. Day, WA, *The Thermodynamics of Simple Materials with Fading Memory*, Springer Tracts in Natural Philosophy, Berlin Heidelberg New York: Springer, 1972
16. Dugdale, DS, Yielding of Steel Sheets Containing Slits, *Journal of the Mechanics and Physics of Solids* 8, 100–104, 1960
17. Eshelby, JD, The Determination of the Elastic Field of an Ellipsoidal Inclusion and Related Problems, *Proceedings of the Royal Society A* 421, 376–396, 1957
18. Foulk, JW, Allen, DH, and KLE Helms, Formulation of a Three Dimensional Cohesive Zone Model for Application to a Finite Element Algorithm, *Computer Methods in Applied Mechanics and Engineering* 183, 51–66, 2000
19. Galileo, G, *Dialogues Concerning Two New Sciences*, New York: Dover, 1636
20. Germain, S, *Recherches sur la théorie des surfaces élastiques*, Paris: Hurard-Courcier, 1821
21. Griffith, AA, The Phenomena of Rupture and Flow in Solids, *Philosophical Transactions of the Royal Society of London A* 221, 163–197, 1920
22. Gurtin, ME, On the Energy Release Rate in Quasi-static Elastic Crack Propagation, *Journal of Elasticity* 9, 187–195, 1979
23. Hashin, Z, Theory of Mechanical Behaviour of Heterogeneous Media, *Applied Mechanics Reviews* 17, 1–9, 1964
24. Hill, R, *The Mathematical Theory of Plasticity*, Oxford: Clarendon, 1950
25. Hill, R, A Self-Consistent Mechanics of Composite Materials, *Journal of the Mechanics and Physics of Solids* 13, 213–222, 1965
26. Navier, CLMH, Memoire sur les lois de l'equilibre et du mouvement des corps solides elastiques, *Mémoires de l'Académie Royale des Sciences* 7, 375–394, 1827
27. Isaac Newton, I, Bernard Cohen and Anne Whitman, *Principia*, Mathematical principles of Natural Philosophy, University of California Press, pp. 994, 1999

28. Phillips, ML, Yoon, C, and DH Allen, A Computational Model for Predicting Damage Evolution in Laminated Composite Plates, *Journal of Engineering Materials and Technology* 21, 436–444, 1999
29. Rice, JR, A Path Independent Integral and Approximate Analysis of Strain Concentration by Notches and Cracks, *Journal of Applied Mechanics* 35(2), 379–386, 1968
30. Searcy, CR, A Multiscale Model for Predicting Damage Evolution in Heterogeneous Media, Ph.D. Thesis, Texas A&M University, 2004
31. Timoshenko, SP, *History of Strength of Materials*, New York: McGraw-Hill, 1972
32. Vakulenko, AA, and ML Kachanov, Continuum Model of Media with Cracks, *Mekhanika Tverdogo Tela* 4, 159–166, 1971
33. Yoon, C and DH Allen, Damage Dependent Constitutive Behavior and Energy Release Rate for a Cohesive Zone in a Thermoviscoelastic Solid, *International Journal of Fracture* 96, 56–74, 1999
34. Zocher, MA, Allen, DH, and SE Groves, A Three Dimensional Finite Element Formulation for Thermoviscoelastic Orthotropic Media, *International Journal for Numerical Methods in Engineering* 40, 2267–2288, 1997